

# Integrated Microwave Photonic Signal Generation System based on the External Modulation Technique

Robinson Guzman<sup>1</sup>, Alberto Zarzuelo<sup>2</sup>, Jessica César<sup>1</sup>, Muhsin Ali<sup>1</sup>, Jean-Raphael Fernández<sup>2</sup>, Oscar Valles<sup>2</sup>, Miguel Virseda<sup>2</sup>, Fernando Martín<sup>2</sup>, Luc Augustin<sup>3</sup> and Guillermo Carpintero<sup>1</sup>

<sup>1</sup>Universidad Carlos III de Madrid, 28911 Leganés, Madrid, Spain

<sup>2</sup>SENER Aeroespacial, 28760 Tres Cantos, Madrid, Spain

<sup>3</sup>SMART Photonics, 5656 AE Eindhoven, The Netherlands

e-mail: [rcguzman@ing.uc3m.es](mailto:rcguzman@ing.uc3m.es); [guiller@ing.uc3m.es](mailto:guiller@ing.uc3m.es);

## ABSTRACT

We present the first photonic integrated circuit for microwave photonic application, implementing signal generation based on the external modulation technique. The quality of the signal is determined by the reference oscillator, which is multiplied by a factor of 2.

**Keywords:** Microwave photonics, Photonic integrated circuits, Mach-Zehnder modulator.

## 1. INTRODUCTION

Microwave Photonics (MWP) has evolved from the combination of photonics and radiofrequency engineering, to exploit the best of both in the generation, transmission and signal processing of high frequency signals, starting at the microwave range (3 GHz to 30 GHz), which has evolved to include the millimeter (30 GHz to 300 GHz) and above. From the photonic side, MWP benefits from large modulation bandwidths (up to 100 GHz), ultrabroad frequency tuning ranges (up to 1 THz) and the low transmission loss of optical fibers (0.1 dB/km) when compared to conventional coaxial cables [1]. More recently, to improve energy-efficiency, flexibility, and scalability, and enable high volume application, the use of photonic integration technology for MWP is opening the field of Integrated Microwave Photonics (iMWP) [2].

One of the key areas of research is the development of suitable photonic signal sources to drive these systems. To date, different signal generation techniques have been proposed to take advantage of the fiber optic distribution of radiofrequency signals, among them are optical heterodyne and optical pulsed source techniques. The former is usually preferred since is comparatively simple, requiring just a couple of free-running laser sources coupled through an optical coupler, and a high-speed photodetector (HS-PD). The radio-frequency signal generated at the HS-PD is given by the wavelength difference between the two laser sources, and if one or both lasers are wavelength tunable, the frequency can be adjusted to any value within a broad range of up to 1 THz [3]. However, as we have also shown, this method of optical heterodyning suffers from poor frequency stability and large phase noise even when both lasers are monolithically integrated on the same chip. Optical linewidths of the individual lasers around tens-of-MHz [5] and the lack of phase correlation between the two leads to considerable instability of the heterodyne mmW/THz signal that limits the practical use. Therefore, locking techniques must be used [4].

An alternative approach is to use a different photonic signal source to achieve the optical heterodyne signal. One such approach is external modulation (EML) of a continuous-wave laser. This technique requires a continuous-wave laser followed by a Mach-Zehnder modulator, which is driven by a continuous-wave electronic source. The key advantage of this technique is that the phase noise of the generated photonic RF signal is directly related to the phase noise of the electronic source. When the modulator is biased to a minimum transmission point and modulated with an RF signal at a frequency of  $f_{LO/2}$  while suppressing the optical central wavelength  $\lambda_0$ , the output optical signal from the modulator is an optical suppressed carrier double sideband (SC-DSB) signal. To the best of our knowledge this paper presents the first integrated microwave photonic circuit implementing signal generation based on the external modulation technique.

## 2. DEVICE DESCRIPTION

The PIC is designed using a generic approach for InP-based PICs and fabricated within a multi-project wafer (MPW) run by SMART Photonics, where standardized building blocks [6] are provided for the selection of the optical components which form photonic transmitter source structure. The PIC as presented in Fig. 1 is composed of

DBR laser, Mach-Zehnder interferometer (MZM), boost amplifier, multimode interference (MMI) couplers, RF photodiode (PD), RF access tracks and straight/bent passive waveguides. The DBR laser structure is formed by a gain section and two mirrors located at the front and rear part of laser, The MZM interferometer structure has two arms in which one of the arms has a DC phase modulator (PM) whilst the other arm has an RF PM. The RF PM arm allows us to inject an RF signal for the modulation of the optical signal supplied by the DBR laser. As for the DC PM is used for the setting of the MZM's biasing point, performing one of the four working points of the MZM's transfer function – Null point, Maximum point, and  $+Q/-Q$  point.

The MZM output is followed by a 1x2 MMI optical splitter. One output port of the MMI is connected to a booster amplifier formed by and Semiconductor Optical Amplifier (SOA) and its output is connected to an internal RF PD. The booster helps us to increase the optical power at the MMI's output port and injected into the RF PD. The RF PD is used as optical-electrical converter to monitor the electrical signal generated when the optical wavelength is modulated by the external RF signal. The outgoing light of the MMI output port is carried through a straight waveguide and ended with  $7^\circ$  angle waveguide. Therefore, in order to reduce any back-reflections at the edges of the chip facet, angled output waveguides and anti-reflection (AR) coating are used as well.

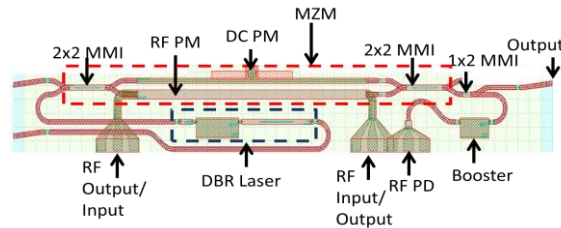


Fig. 1. Layout of the Photonic Integrated Microwave Generator.

### 3. EXPERIMENTAL RESULTS

For the characterization of the PIC, firstly, is mounted on a submount. The electrical pads for the DC-PM and DBR laser are wire-bonded to individual DC tracks on the submount. As we are limited by the RF access tracks on the submount, the signal pads of each GSG RF access of the RF-PM is wire-bonded to each individual RF track on the submount only. The submount is mounted on a temperature-controlled cooper chuck and the chip is temperature stabilized at  $14^\circ\text{C}$  by a thermo-electric cooler (TEC). In this experiment both the internal PD and the booster are not connected, so an external PD with  $-3$  dB bandwidth is up to  $50$  GHz is used. A lensed fiber aligned with the angled waveguide at the chip facet is used for collecting light from the chip output port assuming  $6$  dB of fiber coupling losses. For the DC characterization of the MZM structure the experimental setup used is shown in Fig. 2(a). Each arm of the MZM is reverse biased using voltage sources while the laser is forward biased using a current source. The current injected into the laser is set to  $30$  mA generating an optical wavelength at  $1547.44$  nm. First, for the DC-PM characterization of the MZM, the  $V_{\text{RF-PM}}$  is set to  $0$  V whilst the reverse biasing voltage injected into the DC-PM is sweep from  $0$  to  $9$  V, achieving an extinction ratio of about  $22.3$  dB. The biasing point in null mode and the measured  $V_\pi$  are about  $-5.42$  V and  $8$  V, respectively. Secondly, for the RF-PM characterization, the  $V_{\text{DC-PM}}$  is set to  $0$  V whilst the reverse biasing voltage injected into the RF-PM is sweep from  $0$  to  $9$  V, achieving an extinction ratio of about  $18.1$  dB. The biasing point in null mode and the measured  $V_\pi$  are about  $-4.18$  V and  $8$  V, respectively.

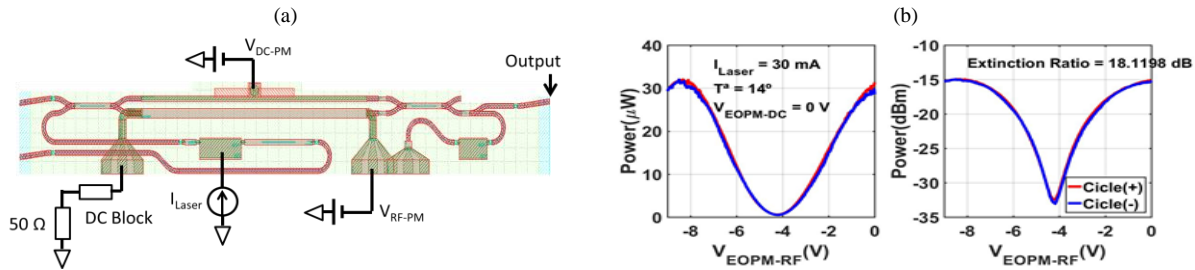


Fig. 2. (a) Experimental Setup for the DC Characterization of the MZM structure. (b) MZM's Transfer Function Response sweeping  $V_{\text{RF-PM}}$  from  $0$  to  $-9$  V and fixing  $V_{\text{DC-PM}}$  to  $0$  V. The plots are shown in linear (left) and Log (right) scale.

The transfer function of the MZM under the last condition measured in both linear and logarithmic scale is shown in Fig. 2(b). For the microwave signal generation, the experimental setup used is shown in Fig. 3(a). As we can see in Fig. 3(a), the RF input of the RF-PM is connected to a DC block and followed by an external RF signal generator. An SMD 50  $\Omega$  resistor for matching of the RF signal is connected to the other end of the RF-PM. In order to achieve the second harmonic generation of the external RF signal injected into the RF-PM input, the DC\_PM must be biased at null point mode (minimum transmission point). The RF power injected into the RF-PM is about 10 dBm with a frequency of 500 MHz. The electrical response measured at the external PD is shown in Fig. 3(b). As we can see, the second harmonic is achieved with an extinction ratio with respect to the fundamental signal is about 12 dB.

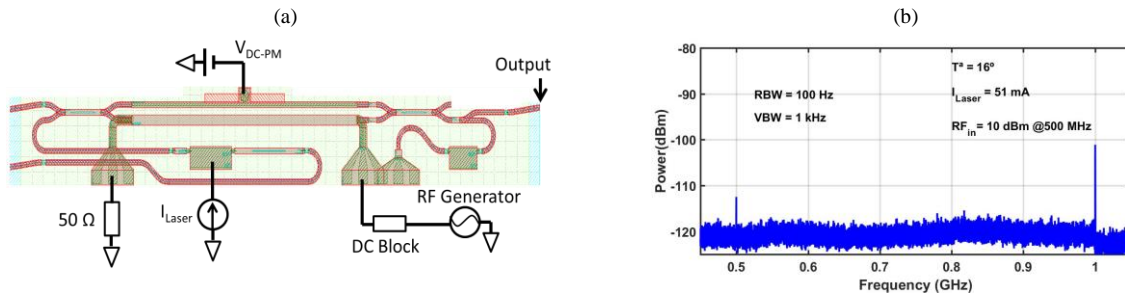


Fig. 3. (a) Experimental Setup for the External Modulation System. (b) Electrical Response biasing the DC-PM at the Null Point.

#### 4. CONCLUSIONS

To the best of our knowledge we present for the first time a photonic integrated circuit for signal generation, based on the external modulation technique, including a semiconductor laser, optical modulator and photodiode on a single chip. We demonstrate that optical carrier suppress double sideband modulation allows us to multiply the RF signal injected into the device, doubling the output frequency. Due to low frequency probe accesses, this demonstration is limited to 500 MHz RF input. The 1 GHz signal on the photodiode inherits the quality of the signal from this reference oscillator and the power level can be furtherly improve with properly RF probes.

#### ACKNOWLEDGEMENTS

This work has been supported by Spanish Ministerio de Economía y Competitividad through Programa Estatal de Investigación, Desarrollo e Inovación Orientada a los Retos de la Sociedad (grant iTWIT, TEC2016-76997-C3-3-R), and by Comunidad de Madrid through Ayuda para la realización de doctorados Industriales ref. IND 2018/TIC-9617.

#### 5. REFERENCES

- [1] Nagatsuma, T., G. Ducournau, et al. (2016). "Advances in terahertz communications accelerated by photonics." *Nature Photonics*, **10**(6): 371-379.
- [2] Marpaung, D., J. P. Yao, et al. (2019). "Integrated microwave photonics." *Nature Photonics* vol. **13**(2). 80–90.
- [3] Lo, M. C., A. Zarzuelo, et al. (2018). "Monolithically Integrated Microwave Frequency Synthesizer on InP Generic Foundry Platform." *Journal of Lightwave Technology* **36**(19): 4626-4632.
- [4] Lo, M. C., S. Jia, et al. (2019). "Foundry-Fabricated Dual-DFB PIC Injection-Locked to Optical Frequency Comb for High-Purity THz Generation." *Optical Fiber Communications Conference and Exhibition*.
- [5] Balakier, K., M. J. Fice, et al. (2014). "Monolithically Integrated optical Phase Lock Loop for Microwave Photonics." *Journal of Lightwave Technology*, **32**(20): 3893-3900.
- [6] Smit, M., X. Leijtens, et al. (2012). "A Generic Foundry Model for InP-based Photonic ICs." *Optical Fiber Communication Conference (OFC)/National Fiber optic Engineers Conference (NFOEC) – 2012 Optical Society of America (OSA) Technical Digest*.